

SIMULATION OF DAMAGE IN RC FRAMES WITH VARIABLE AXIAL FORCES

MARÍA ELENA PERDOMO^{1,2,†}, ANGELA RAMÍREZ^{1,†} AND JULIO FLÓREZ-LÓPEZ^{1,*,‡}

¹ *Universidad de Los Andes, Facultad de Ingeniería, Mérida, Venezuela*

² *Universidad Centro-Occidental Lisandro Alvarado, Barquisimeto, Venezuela*

SUMMARY

The purpose of this paper is to describe how the methods and concepts of continuum damage and fracture mechanics can be applied to the modelling of the hysteretic behaviour of Reinforced Concrete (RC) frame members under variable axial loads. A frame member is considered as the assemblage of an elastic beam-column and two inelastic hinges, as in conventional nonlinear analysis of RC frames. As a result of the combination of damage mechanics and standard RC theory, a simplified model of damage is proposed and implemented as a finite element (FE). This new element can be used with any non-linear commercial FE program. The numerical simulation of several experiments, for which data were available in the literature, verifies the accuracy of the model. Copyright © 1999 John Wiley & Sons, Ltd.

KEY WORDS: reinforced concrete; damage mechanics; variable axial forces; finite elements; non-linear frame analysis

1. INTRODUCTION

The modelling of the behaviour of RC elements under flexural effects and variable axial loads has received relatively little attention.¹ In References 2–4, the technique called ‘shifting of the primary curve’ has been used to take into account variable axial forces with bending moments in shear walls. In References 5 and 6, a triaxial spring model has been proposed that can simulate varying axial force and stiffness degradation. However, still most of the best-known computer programs of frame analysis do not take into account the influence of variable axial loads on the strength properties of the elements. There are also relatively few experimental studies on the subject.^{7–9}

On the other hand, it has been observed that variable axial loads induce modifications in the hysteretic behaviour of the RC elements that are qualitatively and quantitatively as important as other well-studied effects (pinching, low cycle fatigue, unsymmetrical cross-sections, p - δ effects,

* Correspondence to: Julio Flórez-López, Facultad de Ingeniería, Av. Tulio Febres Cordero, Mgrida 5101, Venezuela.
E-mail: iflorez@ing.ula.ve

† Graduate student

‡ Professor

Contract/grant sponsor: CDCHT of the University of Los Andes
Contract/grant sponsor: CDCHT of the Lisandro Alvarado University
Contract/grant sponsor: CONICIT of Venezuela

etc.). In multistorey frames, the axial loads resisted by the columns can experience considerable changes during earthquakes or winds. In Reference 10, the representation of the influence of the axial force on the yield condition is mentioned as one of the main characteristics that any realistic model of RC behaviour should have.

The aim of this paper is to present a model of the hysteretic behaviour of RC members and to assess its capacity to represent the damage process of RC elements under variable axial loads. The model itself was first proposed in Reference 11. These constitutive equations combine the methods of fracture mechanics and continuum damage mechanics with the concept of plastic hinge. In this paper, a very simple algorithm for the analysis of members with the aforementioned model under variable axial loads is proposed and evaluated by the numerical simulation of three tests described in the literature. For these examples, a new finite element based on the model and the algorithm was implemented in a commercial computer program of structural analysis.

The paper is organized as follows. In Section 2, the model is described and its dependence with respect to axial load is pointed out. In Section 3, the new finite element, which permits the implementation of the model in conventional structural analysis programs, is presented. The details of the implementation are discussed in an appendix to this paper.¹² Several numerical simulations that correspond to columns under constant or variable axial loads and monotonic or hysteretic lateral displacements are presented in Section 2.4. The results of another numerical simulation of a test, this time on a multistorey frame subjected to earthquake-type solicitations, are described in Section 3.2.

2. A MODEL OF DAMAGE WITH VARIABLE AXIAL FORCES

2.1. Notation

Let us consider a planar frame made of m structural members linked together by n rigid joints. In order to characterize the behaviour of the structure, we use a notation that presents frame theory in the same way as continuum mechanics, i.e. the state of the frame is defined using 'displacement' variables that characterize the movement of the structure, 'deformation' variables that measure its change of shape and 'stress' variables that describe the way in which external forces are distributed among the different elements of the frame. In order to differentiate these variables from their equivalents in continuum mechanics, we use the adjective 'generalized'.

In Figure 1, a member from a frame is isolated. Generalized stresses and deformations are given by the matrices $\{M\}^t = (M_i, M_j, N)$ and $\{\Phi\}^t = (\Phi_i, \Phi_j, \delta)$, respectively, where these terms have the interpretation indicated in Figure 1. It can be noticed that in a rigid-body transformation of the member, the matrix $\{\Phi\}$ is zero and *vice versa*.

These variables are different from the generalized displacements $\{q\}^t = (q_1, \dots, q_6)$ and internal forces $\{Q\}^t = (Q_1, \dots, Q_6)$ whose meaning is indicated in Figure 2. In the literature, matrices $\{M\}$ and $\{\Phi\}$ are said to be expressed in 'local co-ordinates' and $\{Q\}$ and $\{q\}$ in 'global co-ordinates'.

A constitutive model for a frame member can now be defined as the set of equations that relates the generalized stresses with the history of generalized deformations. For instance, in the case of an elastic frame member, the constitutive model can be expressed as

$$\{M\} = \left\{ \frac{\partial W}{\partial \Phi} \right\} = [S^0]\{\Phi\} \quad \text{or alternatively} \quad \{\Phi\} = \left\{ \frac{\partial W^*}{\partial M} \right\} = [F^0]\{M\} \quad (1)$$

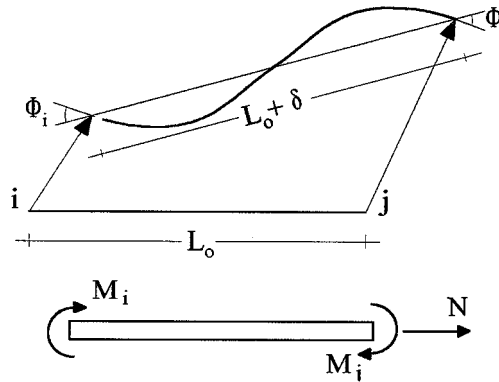


Figure 1. Generalized stresses and deformations for a frame member

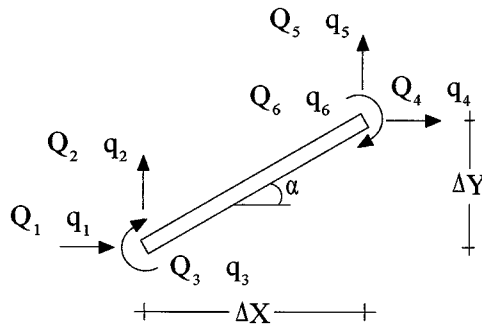


Figure 2. Internal forces and displacements in a frame member

where $[S^0]$ and $[F^0]$ are denoted elastic stiffness and flexibility matrices that may be a function of the axial force N or the generalized stresses $\{M\}$, if geometrical non-linear effects are taken into account. The terms W and W^* are the strain and complementary strain energy.

2.2. State laws of the damage model

Using the same kind of notation described in the preceding section, an inelastic constitutive model for frame members will be presented in terms of 'internal variables', 'state laws' and 'evolution laws'.

Let us consider again a RC frame member between nodes i and j . In order to consider inelastic effects, it will be assumed that energy dissipation is concentrated into special locations called 'inelastic hinges' (see Figure 3). This assumption is conventional in the nonlinear analysis of RC and steel frames.

We postulate now the existence of two sets of internal variables: the generalized plastic deformations $\{\Phi^p\}^t = (\Phi_i^p, \Phi_j^p, 0)$ and the damage $\{D\}^t = (d_i, d_j)$, the latter taking values between

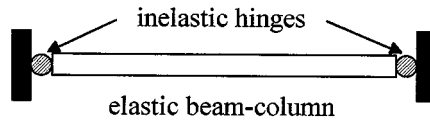


Figure 3. Lumped dissipation model of a frame member

zero and one, so that the stress–deformation relationship for a damaged-elastoplastic member is given by

$$\{\Phi - \Phi^p\} = [F(D)]\{M\}; \quad [F(D)] = \begin{bmatrix} \frac{F_{11}^0}{1-d_i} & F_{12}^0 & 0 \\ F_{21}^0 & \frac{F_{22}^0}{1-d_j} & 0 \\ 0 & 0 & F_{33}^0 \end{bmatrix} \quad (2)$$

where the terms F_{ij}^0 represent the elements of the flexibility matrix introduced in equation (1). Equation (2) can be justified on the basis of concepts of continuum damage mechanics.^{11,13}

The generalized plastic deformations $\{\Phi^p\}$ are the plastic rotations of the inelastic hinges as defined in conventional plastic theories for frames. Physically these variables can be related with the yield of the reinforcement in the case of RC members.

The variables d_i and d_j are damage parameters that measure the state of degradation due to flexural effects in hinges i and j . Physically, these variables can be associated with the level of cracking of concrete.

By inspection of equation (2), it can be noticed that a damage parameter d equal to zero represents a rigid plastic hinge without additional flexibility due to cracking. This is the case of the conventional theory of elastoplastic frames. A damage parameter d equal to one indicates a hinge with infinite flexibility or zero stiffness. In such a case the member has the behaviour of an element with an internal hinge as in the conventional theory of elastic frames. This kind of hinge will be called ‘totally damaged hinge’. This concept is different from the notion of plastic hinge used in conventional perfect elastoplastic frames. The latter case represents a hinge with zero incremental stiffness but infinite stiffness during an elastic unloading. The totally damaged hinges have zero stiffness in any situation.

It is assumed that damage parameters evolve continuously from zero to one, as a function of the loading on the member. In this way, stiffness degradation due to concrete cracking is simulated. It can be noticed that in equation (2), all the inelastic axial effects are being neglected (the last element of matrix $\{\Phi^p\}$ is zero). This assumption has been adopted for the sake of simplicity but it is not an essential hypothesis.

It is evident that equation (2) cannot be considered as a constitutive law (i.e. a relationship between stresses and deformations) because two internal variables were introduced. Therefore, two additional equations must be included. These will be called internal variable evolution laws.

2.3. Evolution laws of the damage model

In order to obtain a plastic deformation evolution law, the yield functions f_i and f_j , one for each inelastic hinge, will be introduced. In continuum damage mechanics, yield functions for damaged materials are introduced on the basis of two concepts: the equivalent stress and the strain

equivalence hypothesis. The former is similar to the concept of equivalent stress of porous media; the latter states that constitutive equations for damaged materials can be obtained from the corresponding laws for intact materials replacing the conventional stress by the equivalent stress.¹⁴ For damaged hinges, an 'equivalent moment' or 'equivalent generalized stress' \tilde{M}_i can be defined as

$$\tilde{M}_i = \frac{M_i}{1 - d_i} \quad (3)$$

By analogy with continuum damage mechanics (strain equivalence hypothesis), the following expression for f_i is proposed:

$$f_i = \left| \frac{M_i}{1 - d_i} - X_i(\Phi_i^p) \right| - K_{i0} \leq 0; \quad X_i(\Phi_i^p) = c_i \Phi_i^p \quad (3)$$

or alternatively

$$f_i = |M_i - (1 - d_i)X(\Phi_i^p)| - (1 - d_i)K_{i0} \leq 0$$

where c_i and K_{i0} can be considered, as a first approximation, as member-dependent constants. The plastic deformation evolution law for hinge i can now be written as

$$\begin{cases} \dot{\Phi}_i^p = 0 & \text{if } f_i < 0 \quad \text{or} \quad \dot{f}_i < 0 \\ \dot{\Phi}_i^p \neq 0 & \text{if } f_i = 0 \quad \text{and} \quad \dot{f}_i = 0 \end{cases} \quad (4)$$

It can be noticed that, for d_i constant, expressions (3) and (4) describe a conventional elastoplastic model with linear kinematic hardening. Plasticity starts, for d_i equal to zero, when the moment reaches the critical value K_{i0} . The plastic hardening is introduced through the term X_i . For d_i constant, the slope of the hardening branch is proportional to the constant c_i . Thus, for constant damage, the model generates a monotonic bilinear envelope.

In the general case (i.e. when damage and plasticity evolve simultaneously), the monotonic envelope is not represented by straight lines because the damage has a softening effect. That is, an increment of damage decreases the stiffness of the member, the value of the plastic limit and the slope of the kinematic hardening term. The 'size' of the elastic domain is therefore the outcome of the competition between the hardening due to plasticity and the softening resulting from damage. In Figure 4, the non-linear envelope described by the model can be appreciated in some force vs. displacement plots.

Before the introduction of the damage evolution law, the equivalent of the concept of 'energy release rate' for an inelastic hinge will be proposed. From expression (2), the complementary strain energy of a damaged member can be defined as

$$W^* = \frac{1}{2} \{M\}^t [F(D)] \{M\} \quad (5)$$

Using this energy as a thermodynamic potential, it is possible to define the forces conjugated to damage for hinges i and j :

$$\{G\}^t = (G_i, G_j) = \left(\frac{\partial W^*}{\partial d_i}, \frac{\partial W^*}{\partial d_j} \right) = \left(\frac{M_i^2 F_{11}^0}{2(1 - d_i)^2}, \frac{M_j^2 F_{22}^0}{2(1 - d_j)^2} \right) \quad (6)$$

The terms G_i and G_j are therefore the equivalent of the 'energy release rate' or 'crack driving force', which is a concept that is defined in fracture mechanics.

Cracking evolution can now be described with a 'generalized Griffith criterion', i.e. there is damage evolution (or cracking extension) if the energy release rate of a hinge reaches a critical value or 'generalized crack resistance', $R(d_i)$. In conventional fracture mechanics, the crack resistance term is assumed to be a function of the crack extension. In the present model, the crack resistance is assumed to depend on the corresponding damage variable:

$$g_i = G_i - R(d_i) \leq 0, \quad \begin{cases} \dot{d}_i = 0 & \text{if } g_i < 0 \quad \text{or } \dot{g}_i < 0 \\ \dot{d}_i > 0 & \text{if } g_i = 0 \quad \text{and } \dot{g}_i = 0 \end{cases} \quad (7)$$

The crack resistance term can be identified on the basis of experimental results. One expression, for RC members, was proposed in Reference 15:

$$R(d_i) = G_{\text{cri}} + q_i \frac{\log(1 - d_i)}{1 - d_i} \quad (8)$$

where G_{cri} and q_i can be considered, again as a first approximation, as member-dependent constants.

2.4. Influence of the axial load

The constants K_0 , c , G_{cr} and q for hinges i and j do not have a clear mechanical meaning. They could be determined in tests on RC members but that would render the model useless for real engineering applications. This is why it is better to compute these constants indirectly via the resolution of the following system of equations:

It is assumed that in a monotonic loading the following conditions apply:

$$M_i = M_{\text{cri}} \Rightarrow d_i = 0 \quad \text{and} \quad g_i = 0 \quad (9a)$$

$$M_i = M_{\text{pi}} \Rightarrow \Phi_i^p = 0; \quad f_i = 0 \quad \text{and} \quad g_i = 0 \quad (9b)$$

$$M_i = M_{\text{ui}} \Rightarrow \Phi_i^p = \Phi_{\text{ui}}^p; \quad \text{and} \quad f_i = 0 \quad (9c)$$

$$M_i = M_{\text{ui}} \Rightarrow dM_i = 0; \quad \text{and} \quad g_i = 0 \quad (9d)$$

where M_{cri} is the cracking moment of the cross section, M_{pi} is the yield moment, M_{ui} is the ultimate moment, Φ_{ui}^p is the plastic rotation that corresponds to the ultimate moment and dM_i indicates an infinitesimal increment of the moment M_i .

Condition (9a) states that damage starts only when the moment on the hinge reaches the cracking moment M_{cri} . This hypothesis allows the computation of the parameter G_{cri} as function of the cracking moment:

$$G_{\text{cri}} = \frac{M_{\text{cri}}^2 F_{11}^0}{2} \quad (10)$$

The last condition (9d) indicates that plots of moment as a function of the damage reach a maximum when the moment on the hinge is equal to the ultimate moment M_{ui} . The relation between moment and damage can be obtained from the equation $g_i = 0$:

$$\frac{M_i^2 F_{11}^0}{2} = (1 - d_i)^2 G_{\text{cri}} + q_i (1 - d_i) \ln(1 - d_i) \quad (11)$$

The search of the critical points of M_i^2 from equation (11) leads to

$$-2(1 - d_u)G_{\text{cri}} + q[\ln(1 - d_u) + 1] = 0 \quad (12)$$

where d_u is the value of damage that corresponds to the ultimate moment. The substitution of this value in equation (11) gives:

$$\frac{M_{ui}^2 F_{11}^0}{2} = (1 - d_u)^2 G_{\text{cri}} + q_i(1 - d_u) \ln(1 - d_u) \quad (13)$$

Equations (12) and (13) constitute a system of two equations that allows the computation of the two unknowns: the parameter q_i and the value d_u .

The second condition (9b) states that plastic deformations begin when the moment on the hinge reaches the yield moment of the member's cross-section. It is also assumed that cracking of the concrete has taken place previously, i.e. $M_{pi} > M_{\text{cri}}$. Thus, equation $g_i = 0$ in this case leads to

$$\frac{M_{pi}^2 F_{11}^0}{2(1 - d_p)} - G_{\text{cri}} - q_i \frac{\ln(1 - d_p)}{1 - d_p} = 0 \quad (14)$$

Expression (14) allows the computation of damage d_p that corresponds to the yielding of the member's cross-section as a function of the yield moment. Now, the condition $f_i = 0$ gives

$$M_{pi} - (1 - d_p)K_{i0} = 0 \quad (15)$$

Equation (15) permits the computation of the parameter K_{i0} .

Finally the third condition (9c) leads to

$$M_{ui} - (1 - d_u)(c_i \Phi_{ui}^p + K_{i0}) = 0 \quad (16)$$

Therefore, the last parameter c_i can be calculated from equation (16). Comparisons between different tests and this model can be found in Reference 11.

It is assumed in this paper that interaction diagrams of M_{cr} , M_p , M_u and Φ_u^p can be computed with good precision for cross-sections of any shape and reinforcement. Specifically, it is assumed that the ultimate plastic rotation can be estimated as

$$\Phi_u^p \cong \chi_p^u \cdot l_p \quad (17)$$

where χ_p^u is the ultimate plastic curvature and l_p an equivalent plastic hinge length.

It is now clear that the parameters K_0 , c , q and G_{cr} are not constants but functions of the axial force N since the cross-section properties M_{cr} , M_p , M_u and χ_p^u also depend on it

$$K_0 = K_0(N); \quad c = c(N); \quad q = q(N); \quad G_{\text{cr}} = G_{\text{cr}}(N) \quad (18)$$

These functions cannot be expressed analytically but can be evaluated for any axial force N by the numerical resolution of equation (9).

Additionally, the equivalent plastic hinge length depends on the moment distribution over the member. In a structural analysis, both axial force and moment distribution may change with time.

A very simple algorithm, that includes the computation of the model's parameters at each iteration, is described in an appendix to this paper.¹²

2.5. Numerical simulations and verification of the model

The model and the algorithm were applied to the simulation of the behaviour of a column with constant cross-section. Figure 4 shows the results of five simulations. In all of these simulations, except the last one, the column was first subjected to a constant axial load and then to a lateral displacement of increasing magnitude. The values of these axial loads were: P equal to zero, P equal to 25 per cent of the balanced load, P equal to the balanced load and P equal to 125 per cent of the balanced load. In the last simulation the axial load and the lateral displacement were increased simultaneously. Specifically, the axial load varied from 0 to 125 per cent of the balanced load.

The model described in Sections 2.2 and 2.3 can be extended to include crack closure effects,¹¹ unsymmetrical cross-sections with different strengths under positive and negative moments,¹¹ low cycle fatigue effects¹⁶ and pinching.¹⁷ None of these generalizations of the model will be discussed in this paper. However, the computer program used in the following simulations was written on the basis of the model described in the present paper and improved by the inclusion of the crack closure effects.

Figure 5 shows the results of two tests on RC columns under compressive axial loads and cyclic lateral displacements conducted at the University of Illinois.⁸ In the test of Figure 5(a), the axial load was kept constant during the test. In the experiment of Figure 5(b), the axial load changed following a complex pattern that included increasing the axial load for negative moments and decreasing it for positive moments. The numerical simulation of both tests is presented in Figure 6. The simplified interaction diagrams used for both simulations are presented in Figure 7.

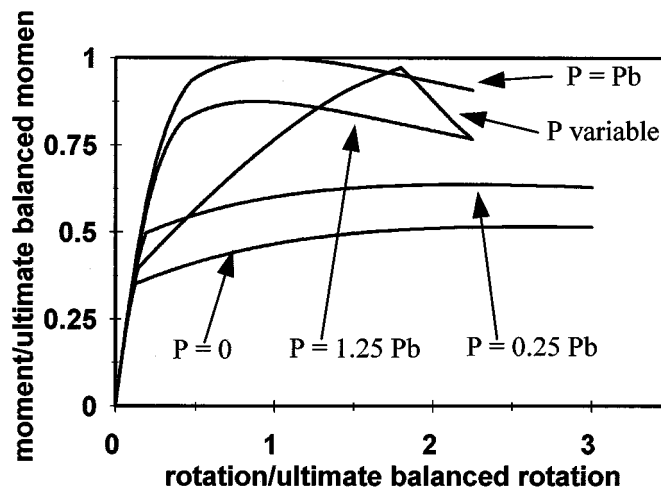


Figure 4. Behaviour of a column after the damage model

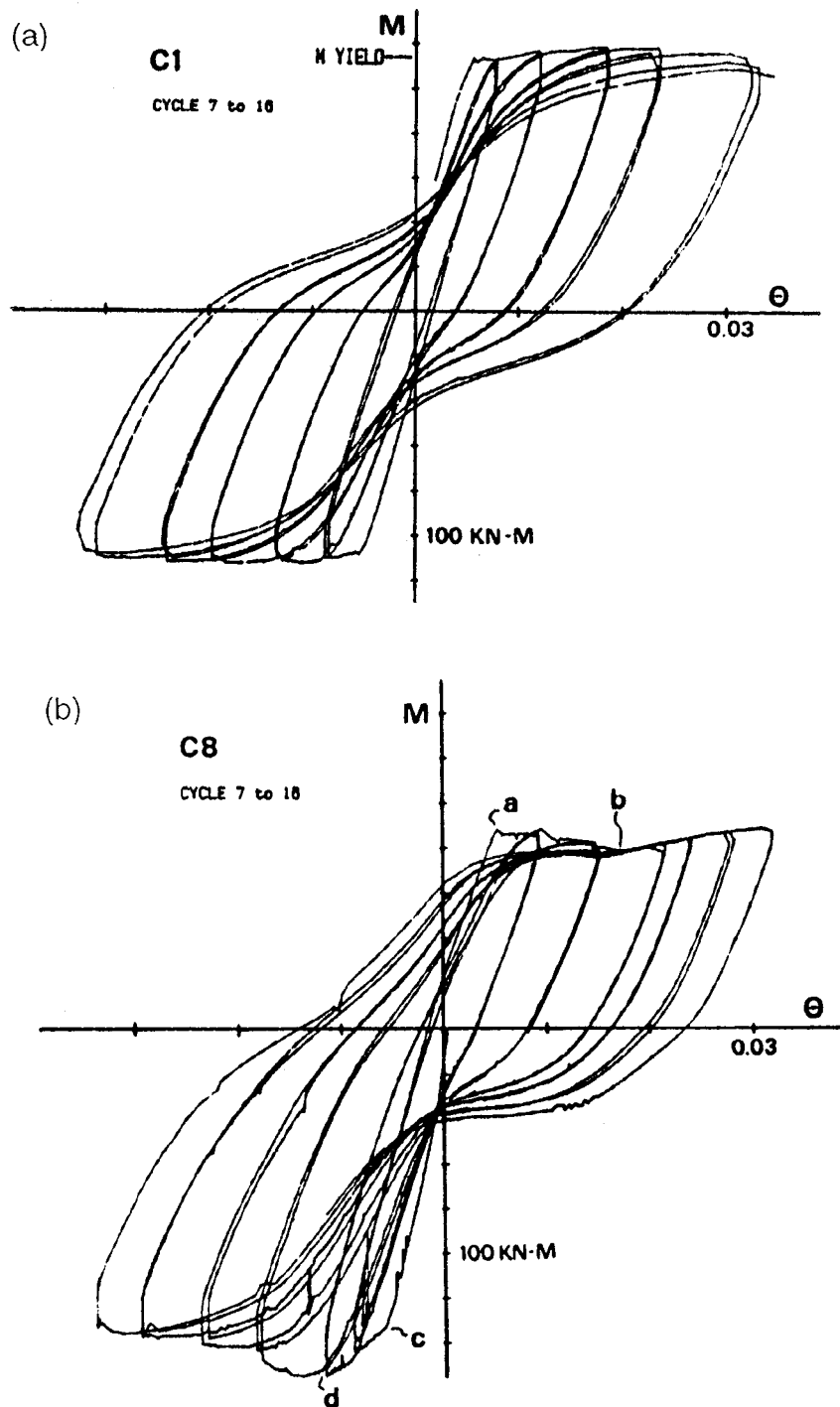


Figure 5. Columns under axial load and cyclic lateral displacements⁸: (a) constant axial load; (b) variable axial load

3. A FINITE ELEMENT FOR RC FRAME MEMBERS UNDER FLEXURE AND AXIAL EFFECTS

3.1. Formulation of the element

The model described in Section 2 can be included in conventional structural analysis programs, as a new finite element. A finite element can be defined as the set of equations that relates the generalized internal forces (nodal forces) $\{Q\}$ with the generalized displacements (degrees of freedom) $\{q\}$ of the element. Therefore, two additional expressions must be added to the constitutive model described in Section 2: On the one hand, the relationship between the generalized member displacements $\{q\}$ and the generalized deformations $\{\Phi\}$, and on the other hand, the relationship between the generalized stresses $\{M\}$ and the internal forces $\{Q\}$. The former will be called 'compatibility equations' and the latter 'member equilibrium equations'. Both sets of equations correspond to well-known concepts in structural mechanics.¹⁸

The compatibility equations have, when geometrical non-linear effects are taken into account, the following expression:

$$\Phi_i = q_3 - (\alpha_0 - \alpha(q)); \quad \Phi_j = q_6 - (\alpha_0 - \alpha(q)); \quad \delta = L(q) - L_0 \quad (19)$$

where

$$\alpha(q) = \text{tg}^{-1} \frac{\Delta Y_o + q_5 - q_2}{\Delta X_o + q_4 - q_1}$$

the terms with the index 'o' represent quantities in the original configuration, and $L(q) = \sqrt{(\Delta Y_o + q_5 - q_2)^2 + (\Delta X_o + q_4 - q_1)^2}$.

Member equilibrium equations can be expressed as

$$\{Q\} = [A(q)]\{M\} + \{I(q)\} \quad (20)$$

where $[A(q)]$ will be called transformation matrix that can be a function of the generalized displacements if geometrical non-linear effects are taken into account:

$$[A(q)]^t = \begin{bmatrix} \frac{\sin \alpha}{L} & -\frac{\cos \alpha}{L} & 1 & -\frac{\sin \alpha}{L} & \frac{\cos \alpha}{L} & 0 \\ \frac{\sin \alpha}{L} & -\frac{\cos \alpha}{L} & 0 & -\frac{\sin \alpha}{L} & \frac{\cos \alpha}{L} & 1 \\ -\cos \alpha & -\sin \alpha & 0 & \cos \alpha & \sin \alpha & 0 \end{bmatrix} \quad (21)$$

where α is the angle between the cord of the element and the axis X and L is the length of the cord. The matrix $\{I\}$ denotes the inertia forces acting on the element. The numerical implementation of this element in a non-linear FE program is described in an appendix to this paper.¹²

3.2. Numerical example

The new finite element has been included^{19,20} in the library of a well-known commercial FE program.²¹ The results of an example analysed using this element are presented in this section. This example corresponds to the numerical simulation of the response of a frame (see Figure 8)

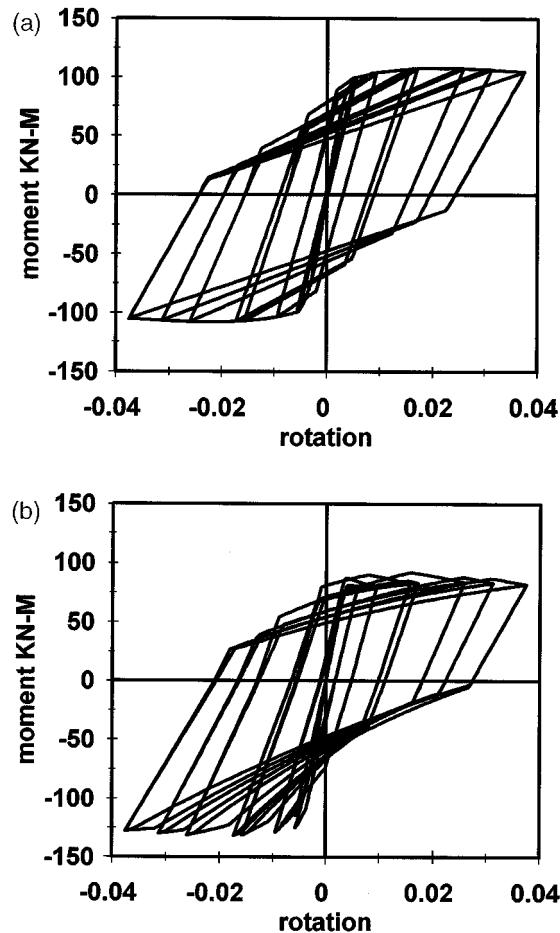


Figure 6. Numerical simulation with the damage model: (a) constant axial load; (b) variable axial load

tested at the University of Illinois, that was subjected to an acceleration history record from the El Centro earthquake.²² The interaction diagrams of the frame elements used in the simulation were computed using standard RC theory²³ and no 'tuning' was allowed. The top displacements observed during the test are shown in Figure 9(a). They can be compared with the computed displacements shown in Figure 9(b).

The computed damage distribution at the end of the event is shown in Figure 10. The maximum values observed in that figure are in the order of 0.5 and correspond to the damage in the columns and beams of the first floor. An important point is the interpretation of these values. It can be noticed that the damage has two kinds of effects in the constitutive laws. The first one is the increase of the flexibility of the member. For instance, the values obtained in the simulation imply reductions in the stiffness coefficients of the beams of the first floor in the order of 10 per cent. The second effect is the reduction of the elastic limit in the yield function of the hinge. The maximum strength of a hinge is obtained when the damage reaches the value d_u defined in

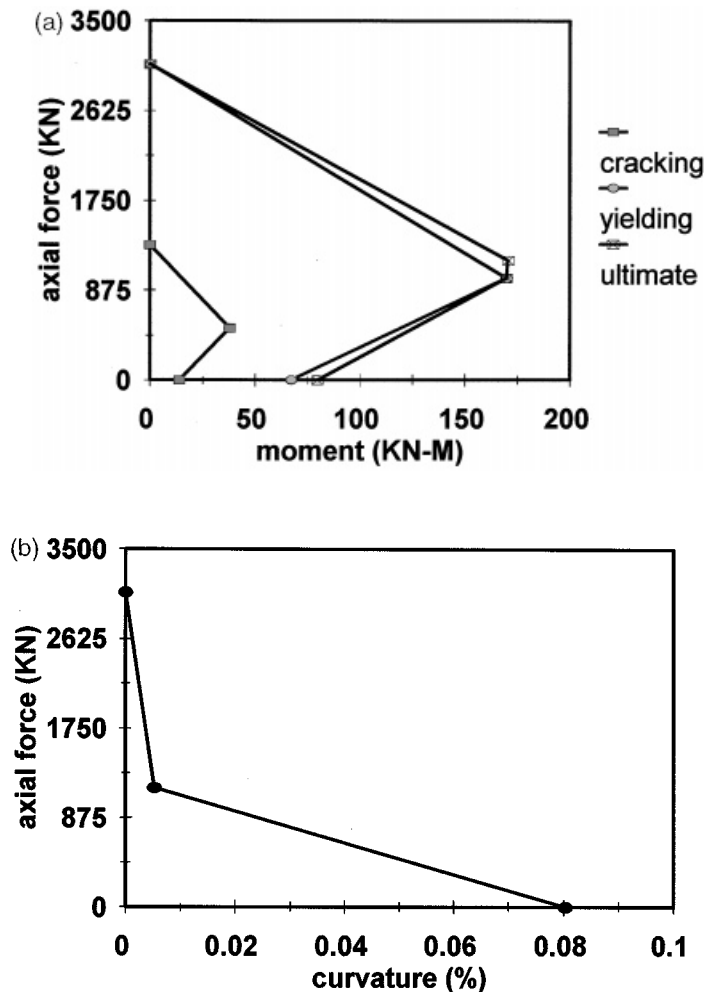
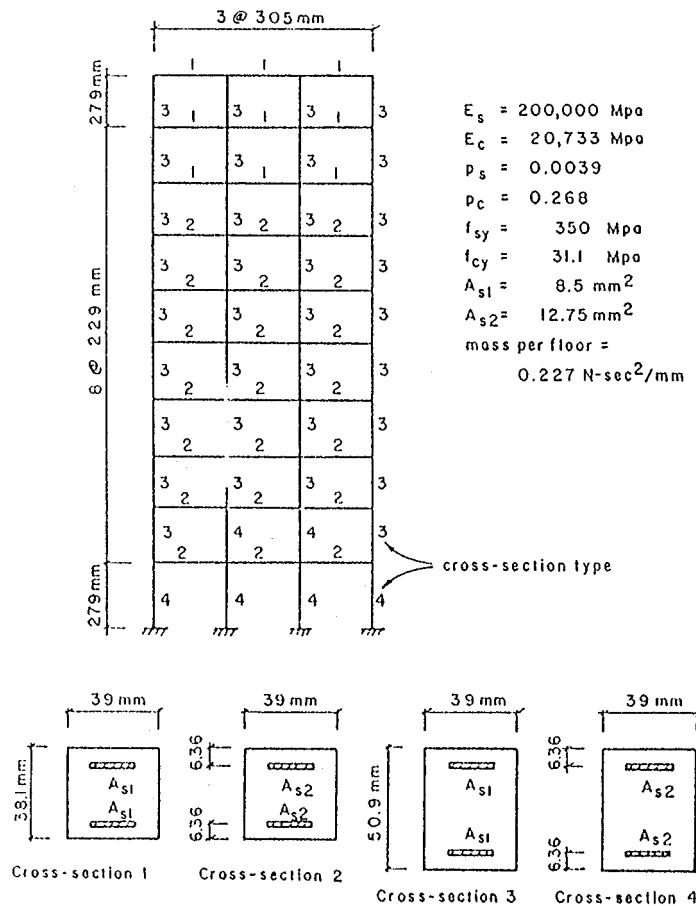


Figure 7. Interaction diagrams used in the simulations

equation (12). That value shows a weak dependence on the axial force. For instance, in the columns of the first floor d_u varies between 0.62 for zero axial force and 0.64 for the balanced force. It can be noticed that the maximum strength of the member was not reached since the damage values at the end of the event are less than d_u . Those results mean that no element of the frame started the softening phase (strength decay) during the analysis. In other words, the simulation predicts that the frame could resist events of higher accelerations.

Figure 11 shows the history of the axial load on one of the exterior columns at the first level of the frame and one of the beams of the first floor. As expected, the axial force on the beam is close to zero. On the other hand, the variation of the axial load on the column is not negligible (the computed balanced load of that member was 43.5 kN) and follows a pattern similar to the one imposed in the test of Figure 5 (see Reference 8).

Figure 8. Multistorey frame tested at Illinois University²²

The plots of moment vs. rotation for a hinge from those elements are shown in Figure 12. In the case of the beam, the hysteretic curve follows a 'quasi-symmetrical' pattern (i.e. with approximately the same apparent properties under positive and negative moments) because the member has a symmetric distribution of the reinforcement. In the case of the column, even if the cross section of the element is symmetric, the curve follows a 'non-symmetrical' pattern due to the variation of the axial load. In this sense, the plot is similar to that computed for a single element shown in Figure 6(b) and also alike to the experimental response observed in Figure 5(b). No softening can be observed in Figure 12 because the damage in the hinge has not reached yet the critical value d_u . However, there is a significant reduction in the stiffness of both elements although this decrease is difficult to appreciate due to the random nature of the rotation at both ends of the elements.

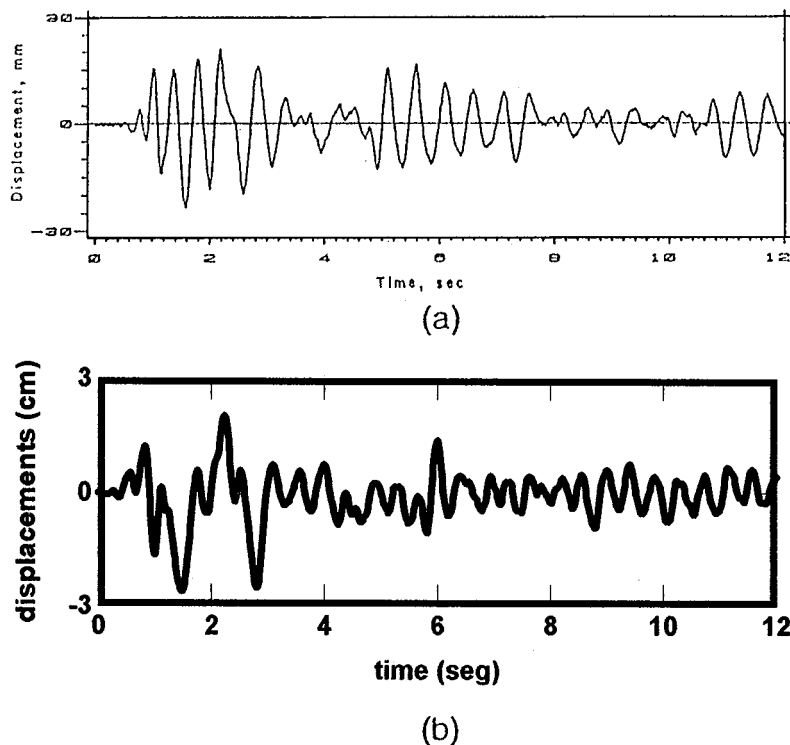


Figure 9. Lateral displacements at the top of the frame: (a) experimental results²²; (b) numerical simulation

4. FINAL REMARKS AND CONCLUSIONS

The results shown in the last two figures confirm that taking into account the variation of the axial load on the strength properties of the elements is very important for a realistic representation of any structural behaviour. If the variation of the axial load is not considered, hysteresis loops of beams and columns would have the same kind of quasi-symmetric shape of Figure 12(a). However, it has been shown in Reference 8 and confirmed by the numerical simulations presented in this paper, that the behaviour of symmetrical columns under earthquake solicitations has many points in common with the response of elements with unsymmetric reinforcement distributions (see Figure 5). That is, an analysis without taking into account this effect would be similar to studying an unsymmetrical element by using the average of the strength properties of the section. It is clear that in both cases, the strength properties are underestimated for a moment of one sign and dangerously overestimated for the moment of the other one.

The model and the finite element proposed in this paper permit the consideration of variable axial load effect in a simple and effective way. During the simulations, a significant increase in the computational cost of the analysis has not been appreciated. The finite element also allows

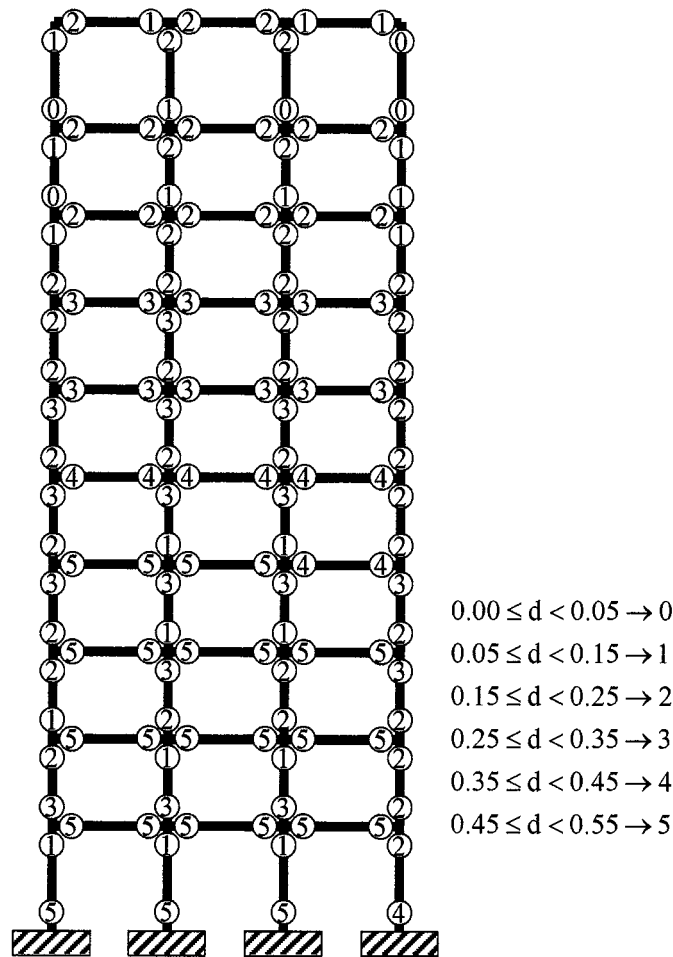


Figure 10. Damage distribution at the end of the simulation

an evaluation of the state of damage of the element. This damage analysis is not performed by a postprocessor, as in the conventional inelastic analysis of RC frames, but during the analysis because the plastic and damage properties of the elements are coupled. The model is based on concepts from standard inelastic analysis of RC members and on the methods of continuum damage and fracture mechanics. It is this last aspect which marks the difference between the present model and other approaches found in the literature.

A point that remains to be developed is the possible relation between the damage values and the serviceability and reparability of the structure. The development of this relationship would require a significant amount of experimental work that would be justified only if the model gains some acceptance among practitioners.

Another point that is frequently raised relates to the advantages of the models based on fracture and damage mechanics concepts over the classic procedures of RC frame analysis. Classic

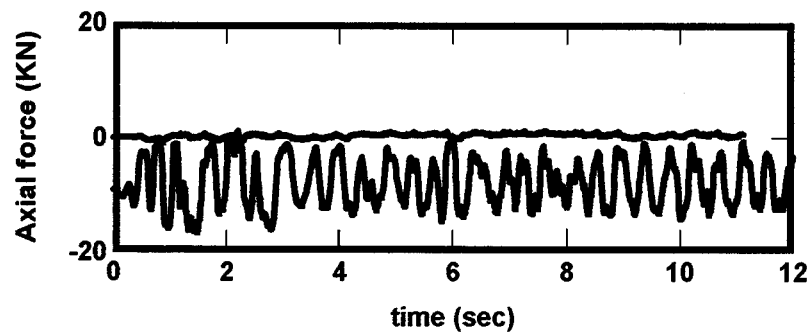


Figure 11. Computed axial loads on a beam and a column

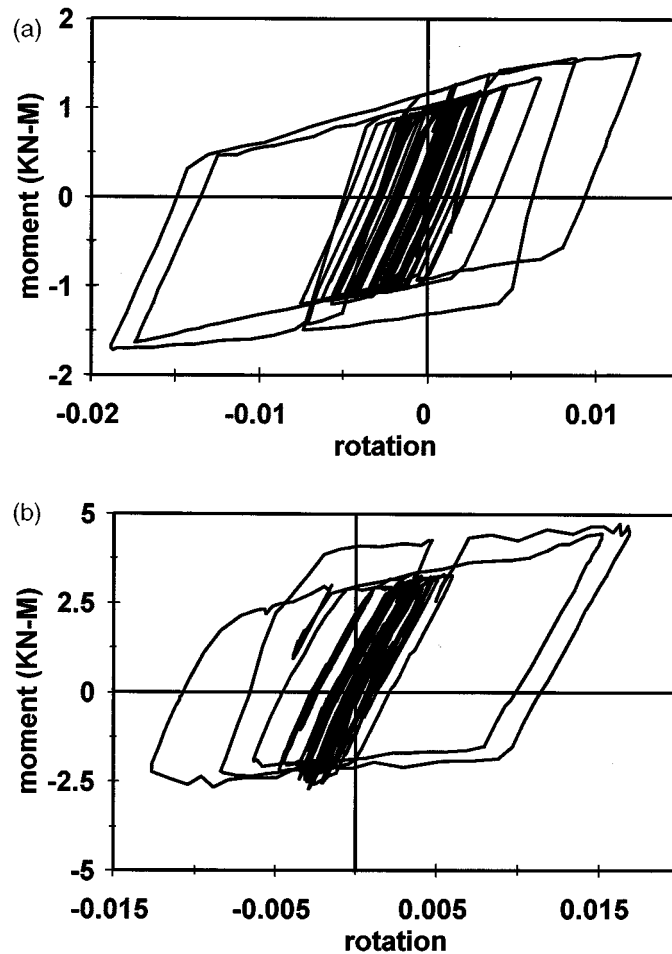


Figure 12. Computed moment-rotation relation: (a) hinge on a beam element; (b) hinge on a column element

models can describe with good precision the observed behaviors, especially if some degree of tuning is allowed. However, the authors think that the use of concepts such as energy release rate, coupled plastic-damage analysis, Griffith criterion and others allow for a more rational and physically sounded description of the damage process in RC frames. More importantly, the same concepts could be used to model more complex behaviors, such as time-dependent damage and three-dimensional frames with coupled biaxial and torsional damage. Perhaps the use of those concepts in these situations would result in a much simpler and accurate description. In any case, the authors believe that damage analysis of RC frames using the plastic hinge concept and the methods of fracture mechanics is an interesting alternative approach that must be explored.

ACKNOWLEDGEMENTS

The results presented in this paper were obtained in the course of an investigation sponsored by the C.D.C.H.T. of the University of Los Andes, C.D.C.H.T. of the Lisandro Alvarado University and CONICIT of Venezuela.

REFERENCES

1. M. S. L. Roufaiel and C. Meyer, 'Analytical modeling of hysteretic behavior of R/C frames', *J. Struct. Div. ASCE* **113**(3), 429–443 (1987).
2. M. Saatcioglu and A. T. Derecho, 'Dynamic inelastic response of coupled walls as affected by axial forces', *Nonlinear Design of Concrete Structures CSCE-ASCE-ACI-CEB International Symposium*, Univ. of Waterloo, Ontario, 7–9 August 1979, pp. 639–670.
3. M. Keshavarzian and W. Schnobrich, 'Computed nonlinear seismic response of R/C wall-frame structures', Civil Engineering Studies, Structural Research Series No. 515, University of Illinois, Urbana, 1984.
4. T. Takayanagi and W. Schnobrich, 'Computed behavior of reinforced concrete coupled shear walls', Civil Engineering Studies, Structural Research Series No. 434, University of Illinois, Urbana, 1976.
5. S. S. Lai, G. T. Will and S. Otani, 'Model for inelastic biaxial bending of concrete members', *J. Struct. Engng. ASCE* **110**(11), (1984).
6. S. S. Lai and G. T. Will, 'R/C space frames with column axial force and biaxial bending moment interactions', *J. Struct. Engng. ASCE* **112**(7), (1986).
7. N. D. Gilberstsen, J. P. Moehle, 'Experimental study of small-scale RC columns subjected to axial and shear force reversals', Structural Research Series No. 481, Civil Engineering Studies, University of Illinois, Urbana, July 1980.
8. D. P. Abrams, 'Influence of axial force variations on flexural behavior of reinforced concrete columns', *ACI Struct. J.* (1987).
9. S. N. Bousias, G. Verzeletti, M. N. Fardis and E. Gutierrez, 'Load-path effects in column biaxial bending with axial force', *J. Engng. Mech. ASCE* **121**(5), (1995).
10. K. J. Mørk, 'Stochastic analysis of reinforced concrete frames under seismic excitation', *Soil Dyn. Earthquake Engng.* **11**, 145–161 (1992).
11. J. Flórez-López, 'Unilateral model of damage for RC frames', *J. Struct. Engng. ASCE* **121**(12), (1995).
12. M. E. Perdomo, A. Ramírez and J. Flórez-López, Appendix to simulation of damage in RC frames with variable axial forces. http://www.cecalc.ula.ve/areas_trabajo/investigadores/publicaciones/jflorez-anexo.zip
13. J. Flórez-López, 'Frame analysis and continuum damage mechanics', *J. Eur. Mech.* **17**(2), (1998).
14. J. Lemaitre, *A Course on Damage Mechanics*, Springer, Berlin, 1992.
15. A. Cipollina, A. López-Inojosa and J. Flórez-López, 'A simplified damage mechanics approach to nonlinear analysis of frames', *Comput. Struct.* **54**(6), 1113–1126 (1995).
16. E. Thomson, A. Bendito and J. Flórez-López, 'Simplified model of low cycle fatigue for RC frames', *J. Struct. Engng. ASCE* **124**(9), (1998).
17. J. Flórez-López and C. Quintero-Febres, 'Modelado de la degradacion de adherencia en elementos de concreto armado sometidos a cargas cíclicas', *Int. Conf. on Numerical Methods in Engineering and Applied Sciences (CIMENICS 98)*, Puerto Ordaz, Venezuela (1998).
18. H. G. Powell, 'Theory of nonlinear elastic structures', *J. Struct. Div. ASCE* **95** (ST12), 2687–2701 (1969).
19. A. Ramírez, 'Análisis Dinámico con modelos histeréticos de daño', *Thesis*, University of Los Andes, Mérida, Venezuela, 1995 (in Spanish).

20. M. E. Perdomo, 'Un modelo histeretico de daño con fuerza axial variable', *Thesis*, University of Los Andes, Mérida, Venezuela, 1997 (in Spanish).
21. ABAQUS, User's Manual, Hibbitt, Karlsson and Sorensen, Inc., 1997.
22. T. J. Healey and M. A. Sozen, 'Experimental study of the dynamic response of a ten-story reinforced concrete frame with a tall first story', Structural Research Series No. 450, University of Illinois, Urbana III, 1978.
23. R. Park and T. Paulay, *Reinforced Concrete Structures*, Wiley, New York, 1975.